

BRITTLE OR QUASI-BRITTLE FRACTURE OF CERAMIC NANOCOMPOSITES UNDER DYNAMIC LOADING

Evgeniya G. Skripnyak¹, Vladimir V. Skripnyak¹, Vladimir A. Skripnyak^{1,2},

Nataliya V. Skripnyak^{1,3}, and Irina K. Vaganova¹

¹ National Research Tomsk State University
36 Lenin Avenue, 634050 Tomsk, Russia
e-mail: skrp@ftf.tsu.ru

² Institute of Strength Physics and Materials Sciences SB RAS
2/4, pr. Akademicheskii, Tomsk, 634021, Russia
e-mail: skrp2006@yandex.ru

³ Linköping University
Linköping, SE-581 83 Sweden
e-mail: natali.skrp@mail.ru

Keywords: Mechanical Properties, Nanostructured Ceramics, Dynamic Loading, Fracture.

Abstract. *Multiscale computer simulation was used for simulation of the damage nucleation and fracture of $ZrB_2 - ZrO_2$, $ZrB_2 - B_4C$, $Al_2O_3 - ZrO_2 - Y_2O_3$, $Al_2O_3 - B_4C$ nanocomposites under dynamic loading. The aim of research was the study transition from brittle to quasi-brittle fracture of nanocomposites under dynamic loading. It was shown that isolated micro- and mesoscale cracks can be nucleate in ceramic nanocomposites near voids under stress pulse amplitude less than the Hugoniot elastic limit. The critical fracture stress on mesoscale level depends not only on relative volumes of voids and particles concentration, but also sizes of corresponding structure elements. Results of simulation have shown the Hugoniot elastic limit and ceramics damage kinetics under dynamic loading depends on a volume concentration of nano-particles and nano-voids clusters.*

1 INTRODUCTION

Ceramic nanocomposites constitute an important class of constructional materials for high temperature applications in the aerospace industry: hypersonic re-entry vehicles, rocket nozzle inserts, and cutting tools, wear resistant parts etc. Thus, for designing materials and predicting the destruction of new ceramic composites for engineering applications need an adequate theoretical model that can be used in computer simulation.

In the present paper, we propose a computational model to predict the strength of quasi-brittle nanocomposites such as $ZrB_2 - ZrO_2$, $ZrB_2 - B_4C$, $Al_2O_3 - ZrO_2 - Y_2O_3$, $Al_2O_3 - B_4C$

in wide range of strain rates. Considered nanocomposites are a class of the ultra-high temperature ceramics (UHTC).

The matrix of UHTC composites make up 15 boride, carbide and nitride compounds which have the melting temperature above 3250 K [1]. These compounds are brittle at low homologous temperatures and demonstrate not high enough strength and toughness at quasi-static and dynamic loading.

New UHTC nanocomposites possess enhanced strength and fracture toughness at quasi-static loading [2]. Effective way to increase strength UHTC is the creation on their base nanocomposites containing the ceramic nano-sized particles, graphite flakes, carbon fibres, and metal or ceramic whiskers. Mechanical behaviour of UHTC composites under intensive dynamic loadings is not well understood.

2 MODEL OF MECHANICAL BEHAVIOR OF NANOCOMPOSITES

Mechanical properties of nanocomposites based on refractory compounds depend not only on their structure and composition, but also on the manufacturing technology. High-temperature isostatic pressing UHTC composites occurs at temperatures above 1500 K, while the temperature at selective laser sintering or sintering spark plasma is above 2000 K.

When the ceramic composite is cooled from sintering temperature to room temperature, residual stresses arise around inclusions of strengthening phases. Residual stress and bulk defects in the structure have a negative impact on strength properties of ceramic products.

Residual stresses have to be considered while predicting the mechanical behaviour of ceramic materials under external impacts.

Residual pressure around the particle can be calculated by the formula [3]:

$$p_{res} = [(\alpha_m - \alpha_{inc})(T - T_r)E_m E_{inc} \left(\frac{d}{r + d}\right)^3] / [E_{inc}(1 - 2\nu_m) + 2E_m(1 - 2\nu_{inc})], \quad (1)$$

where p_{res} is the residual pressure, α_m , α_{inc} are the linear thermal expansion coefficients of matrix and inclusion, respectively, T is the sintering temperature, and T_r is the room temperature, d is the particle diameter, r is the distance from the surface of particle E_m , E_{inc} , are the Young's moduli of matrix and inclusions, and ν_m , ν_{inc} are the Poisson's ratios of matrix and inclusions, respectively.

The calculated residual stresses in ZrB_2 matrix composites and different ceramic inclusions shown in Figure 1. Residual pressures were obtained for the difference between the sintering temperature and the room temperature ~1500 K.

Note, the residual pressures can have a different sign for various inclusions. Residual pressures can causes local tensile or compression of matrix near the particle. If the residual stresses are tensile, the strength of ceramic composites under tension is significantly lower than under compression.

Thus, this effect is advisable to apply for strengthening of nanocomposites using inclusions, which lead the formation positive pressures around nanoparticles.

The value of the residual pressure around the inclusions is less than the Hugoniot elastic limit, but is comparable to the quasi-static tensile strength of ZrB_2 matrix. As shown in Figure 2 the residual pressure lead to changing of the fracture toughness of ZrB_2 matrix composites.

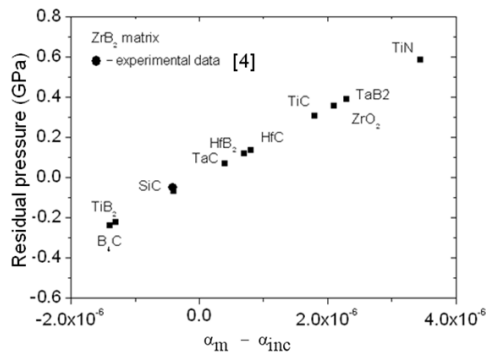


Figure 1. Residual pressure vs the difference between the linear thermal expansion coefficients of matrix and inclusions.

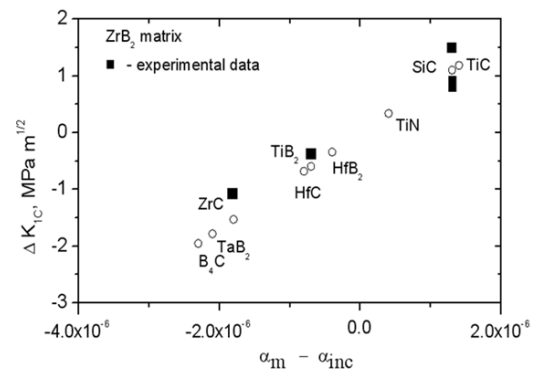


Figure 2. Fracture toughness of ZrB₂ based composites vs the difference between the linear thermal expansion coefficients of matrix and inclusions.

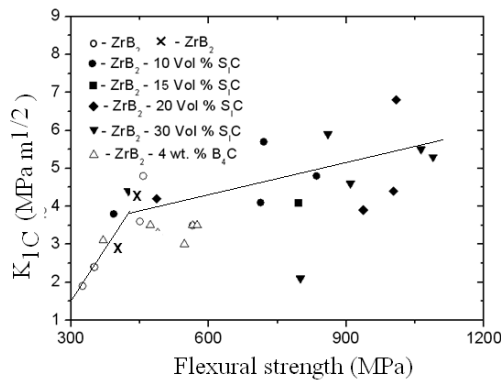


Figure 3. Fracture toughness of ZrB₂ based composites versus flexural strength.

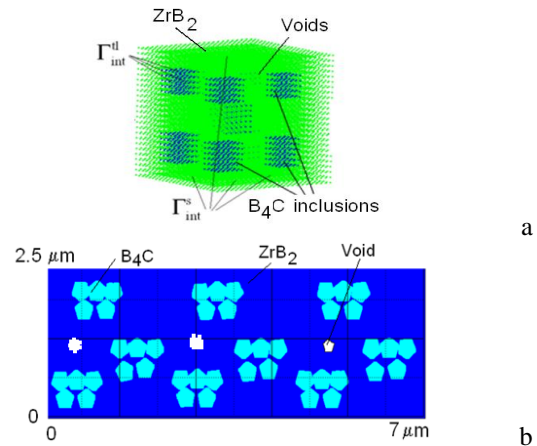


Figure 4. (a) Representative volumes of composites ZrB₂-B₄C with uniform distribution of inclusions. (b) Clusters of inclusions.

The correlation between the fracture toughness and the flexural strength of ZrB₂-B₄C and ZrB₂-SiC composites is shown in Figure 3. Symbols are experimental data [1-4].

When the concentration of inclusions exceeds the percolation threshold (~30 %) the frame structure can be formed in the composites. The scatter of the experimental data shows that the strengthening and toughening of composites is caused not only the residual stress, but also other factors [5].

To study the dynamic strength of UHTC nanocomposites we used the method of multiscale simulation [6-8]. The calculated values of residual stresses were used in the simulation of loading of the elementary volume of ZrB₂ matrix nanocomposite under shock wave loadings.

The mechanical response of the nanocomposites in the amplitude range from 0.8 to 2 of the Hugoniot elastic limit (~15 GPa) was numerically simulated. The Hugoniot elastic limit of ZrB₂ ceramics with a porosity of ~7 % is equal to 7.11 GPa.

The elementary volumes (EV) of nanocomposite materials, used in simulation, are shown in Figure 4. Figure 4a shows the volume with regular distribution of nanoparticles in matrix grain. Figure 4b shows the section of volume with clusters of nanoparticles.

The modified smooth particle hydrodynamics (SPH) method was used for numerical simulation [9]. Smoothed particles with sizes of ~20 nm were used in numerical simulation shock loading of ceramic nanocomposites. Grains of matrix and inclusions had a different mechanical impedances ρC_l (ρ is the mass density, and C_l is the longitudinal sound velocity).

Material parameters for the matrix and inclusions of ceramic nanocomposites are shown in Table 1.

Phase	$\rho, 10^3$ kg/m ³	E, GPa	Poisson Ratio	$\alpha,$ 10^{-6} K^{-1}	$C_l,$ 10^3 m/c	$\mu,$ GPa	$\sigma_{HEL},$ GPa
Al ₂ O ₃	3.97	395.8	0.254	8.8	10.92	156.5	9-14
t-ZrO ₂ (3mol.% Y ₂ O ₃)	6.05	219.0	0.312	12.2	7.07	83.0	8.9-17.0
m-ZrO ₂	5,6	236	0.303	8.0-10.6	7.5	86.4	
ZrB ₂	6.09	450	0.128	5.9-6.5	8.8	212	7.11
SiC	3.22	454	0.163	4.7	11.89	195	13.2-14.7
B ₄ C	2.52	432-463	0.151-0.18	4.5	13.42	188	16.0-17.1

Table 1: Material parameters of ceramic phases.

The impedance ρC_l for ZrB₂, B₄C are: 5.08, 3.55 [$10^7 \text{ kg/m}^2 \text{ s}$], respectively. Therefore, on the mesoscale level, shock waves are reflected from boundaries of matrix and inclusions. In the result, particle velocities, stresses, and temperature can be distributed non-uniformly in the elementary volume of nanocomposite during hundreds nanoseconds.

Mechanical behavior of ceramic matrix and inclusions were described using the model of damaged medium [4–9].

The damage parameter D is determined by the relation [4, 5]:

$$D = \int_0^{t_f} \frac{\dot{\varepsilon}_{eq}^n}{\varepsilon_f^n} dt, \quad (2)$$

where $\dot{\varepsilon}_{eq}^n = [(2/3)\dot{\varepsilon}_{ij}^n \dot{\varepsilon}_{ij}^n]^{1/2}$ denote an intensity of inelastic strain rate tensor, ε_f^n is the threshold of inelastic deformations of material particles (the volumes of the phases at the micro level) at fracture, $\varepsilon_f^n = D_1 (P^* + T^*)^{D_2}$, $T^* = \sigma_{sp}/P_{HEL}$, $P^* = p/P_{HEL}$, P_{HEL} is pressure correspond to the Hugoniot elastic limit, $\sigma_{sp} = (3\rho C_l \dot{\varepsilon}_{eq} K_{1C}^2)^{1/3}$, C_l is the longitudinal sound velocity [9].

The thresholds stress of fracture for ceramic matrix and inclusions under compression in wide range of strain rates can be described by Eq. (3), if the volume concentration of inclusions is less than 30 % and porosity is less than 10 % [10,11].

$$\sigma_f / \sigma_0 = 1 + (\dot{\varepsilon}_{eq} / \dot{\varepsilon}_0)^{2/3}, \quad \sigma_0 = 4.25 K_{1C} \eta^{1/4} / [\alpha]^{1/2}, \quad \dot{\varepsilon}_0 = 4.25 K_{1C} \eta^{3/4} / [\alpha \rho E]^{1/2}, \quad (3)$$

where α is a specific volume of voids, ρ is the mass density, K_{1C} is the fracture toughness, E is the Young's modulus, and η is a square density of unstable microcracks [10, 11].

Note, the fracture toughness of the matrix and inclusions have been corrected for residual stresses.

Averaged in elementary volume of material the threshold stress of fracture is used in Eq (2) for determination of σ_{HEL} .

The following parameters of Eq (3) for ZrB_2 matrix and for B_4C inclusions were used in the calculations:

ZrB_2 : $E=495$ GPa, $\rho=6.11 \cdot 10^3$ kg/m³, $K_{IC}=3.5$ MPa m^{1/2}, $\sigma_{HEL}=7.11$ GPa, $p_{HEL}=3.07$ GPa, $D_I=0.1$, $D_2=1.$, $Cl=9.233$ km/s, $\sigma_{sp}=0.5$ GPa, $\sigma_{sd}=0.5$ GPa,

B_4C : $E=432$ GPa, $\rho=2.52 \cdot 10^3$ kg/m³, $K_{IC}=5$ MPa m^{1/2}, $\sigma_{HEL}=16$ GPa, $p_{HEL}=7.2$ GPa, $D_I=0.1$, $D_2=1.0$, $Cl=12.8$ km/s, $\sigma_{sp}=0.32$ GPa, $\sigma_{sd}=13.2$ GPa.

The Hugoniot elastic limit and the effective sound velocity of composite materials are determined using simulation results of shock wave propagation in the elementary volume of material [6-8].

Using averaged values of sound velocities and the elastic limit of the Hugoniot elastic limit the shear strength of ceramic nanocomposites σ_{sd} can be determined by the relation:

$$\sigma_{sd} = 1.5 \left(1 - \frac{\langle C_b \rangle^2}{\langle C_l \rangle^2} \right) \sigma_{HEL}, \quad (4)$$

where C_b , C_l are the effective bulk sound velocity and the longitudinal sound velocity, respectively, σ_{HEL} is the Hugoniot elastic limit of composites.

3 RESULTS AND DISCUSSION

Calculated values of the equivalent stress in the ZrB_2 matrix versus specific values of shock pressure are shown in Figure 5. The relaxation of the equivalent stress at high strain rates is mainly caused by a nucleation of micro-cracks around pores and inclusions.

Figure 6 shows the nucleation of cracks around voids under shock compression with amplitude of ~ 10 GPa. Initial distribution of B_4C nanoparticles and voids in section of the volume is shown in Figure 4b.

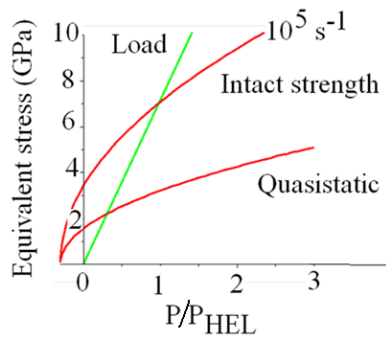


Figure 5. The intact strength and strength for the failed polycrystalline ZrB_2 .

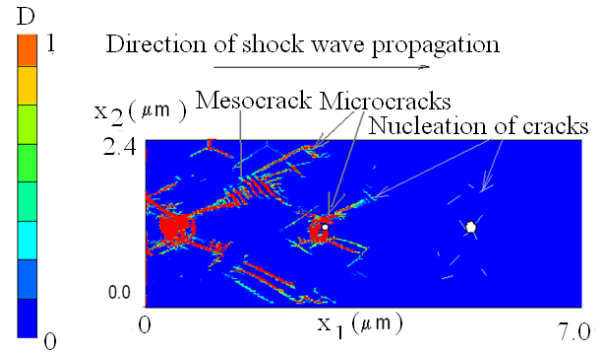


Figure 6. Crack nucleation behind the front of shock wave.

As showed Figure 6, the damage of $ZrB_2 - B_4C$ nanocomposites near voids can be formed under pressure amplitude less than P_{HEL} of matrix. The relaxation of the equivalent stress is associated with cracks nucleation. In consequence of this, the Hugoniot elastic limit of ceramic nanocomposites decreases proportionally to specific volume of voids. Under shock compression stress field around cluster of nano-particles is close to that which occurs near the particle of micron size. Used multiscale model allows considering this phenomenon.

In the considered nanocomposites clusters of inclusions lead to increased resistance to the growth of cracks or even complete stop. As a result the transition from brittle to quasi-brittle fracture of nanocomposites under dynamic loading takes place.

The Hugoniot elastic limits for non-porous nanocomposites were evaluated according to the results of modeling the nucleation of damage in the elementary volume of material under shock compression. Obtained for the ZrB_2 or Al_2O_3 matrix nanocomposites the Hugoniot elastic limits are given in the Table 2.

Volume concentration of inclusions (%)	0	5	10	15	20	25	30
Nanocomposite	Hugoniot elastic limit , σ_{HEL} (GPa)						
$\text{ZrB}_2\text{--B}_4\text{C}$	7.11	7.43	7.8	8.5	9.1	9.55	10.1
$\text{ZrB}_2 - \text{t ZrO}_2$	7.11	7.45	8.9	8.53	9.04	9.4	10.01
$\text{ZrB}_2 - \text{Al}_2\text{O}_3$	7.11	7.30	7.43	7.64	7.9	7.8	7.7
$\text{Al}_2\text{O}_3\text{--ZrO}_2$,	9.1	9.35	9.67	9.9	10.01	10.3	10.4
$\text{Al}_2\text{O}_3\text{--B}_4\text{C}$	9.07	9.36	9.77	10.05	10.65	11.5	11.1

Table 2: Theoretical values of the Hugoniot elastic limit of several ceramic nanocomposites.

In considered groups of composites the Hugoniot elastic limits increase with increasing concentration of nano-inclusions from 0 to 30 %. In considered ZrB_2 matrix nanocomposites the greatest relative increase of the Hugoniot elastic limit is observed at same concentrations of nanoparticles B_4C and ZrO_2 .

In Al_2O_3 matrix nanocomposites the greatest relative increase in the Hugoniot elastic limits was caused by B_4C nanoparticles.

4 CONCLUSIONS

Multi-scale model proposed for computer simulation of the mechanical behaviour of UHTC nanocomposites.

The model allows investigating the effect of structures of nanocomposites on their mechanical properties under dynamic loading.

Model was used for simulation of $\text{ZrB}_2 - \text{ZrO}_2$, $\text{ZrB}_2 - \text{B}_4\text{C}$, $\text{Al}_2\text{O}_3 - \text{ZrO}_2 - \text{Y}_2\text{O}_3$, $\text{Al}_2\text{O}_3 - \text{B}_4\text{C}$ nanocomposites under shock compression with amplitudes from 6 to 15 GPa.

In studied UHTC nanocomposites the dynamic shear strength increases proportionally volume concentration of inclusions in the range up to 30 %.

Model predicts that isolated micro- and mesoscale cracks nucleate in UHTC nanocomposites near voids under stress pulse amplitude less than the Hugoniot elastic limit.

The Hugoniot elastic limits of nanocomposites decrease proportionally to porosity in the range from 0 to 10 %.

ACKNOWLEDGMENT

This work was supported partially by the Grant from the President of Russian Federation, and by a grant from the Foundation of D. I. Mendeleev's National Tomsk State University within the Program of increasing the competitiveness of TSU. The authors are grateful for the support of this research.

REFERENCES

- [1] S.Q. Guo, Densification of ZrB₂-based composites and their mechanical and physical properties, *Journal of the European Ceramic Society*, **29**, 995–1011, 2009.
- [2] J.J. Melendez-Martinez, A. Dominguez-Rodriguez, F. Monteverde et al. Characterisation and high temperature mechanical properties of zirconium boride-based materials, *Journal of the European Ceramic Society*, **22**, 2543–2549, 2002.
- [3] I.A. Stepanov, V.A. Skripnyak, S.P. Andrietz, et.al., *Nuclear physics and engineering*, **2**, 1–10, 2011.
- [4] V.V. Skripnyak, V.A. Skripnyak, I.K. Vaganova, et al. Multiscale simulation of porous quasi-brittle ceramics fracture. *Applied Mechanics and Materials*, **756**, 196–204, 2015.
- [5] V.V. Skripnyak, E.G. Skripnyak, V.A. Skripnyak, and I.K. Vaganova “Computer simulation of fracture quasi-brittle ceramic nanocomposites under pulse loading”, Proc. 11th. World Congress on Computational Mechanics (WCCM XI), edited by Eugenio Oñate, Xavier Oliver and Antonio Huerta, CIMNE Publ., Barselona, Spain, 2014, **IV**, 3904–3914, 2014.
- [6] C. C. Holland and R. M. McMeeking, The influence of mechanical and microstructural properties on the rate-dependent fracture strength of ceramics in uniaxial compression. *International Journal of Impact Engineering*, **81**, 34–49, 2015.
- [7] E. G. Skripnyak, V.A. Skripnyak, and V. V. Skripnyak. Fracture of nanoceramics with porous structure at shock wave loadings, *Shock Compression of Condensed Matter*. AIP Conf. Proc, **1426**, N.Y. 965 –970, 2012.
- [8] E.G. Skripnyak, V.A. Skripnyak, I.K. Vaganova, A.S. Yanyushkin, et. al., *Izvestiya Vuzov. Physica*, (in Ruassian), **55**, (7/2), 119–123, 2012.
- [9] E.G. Skripnyak, V.V. Skripnyak, I.K. Vaganova, and V.A. Skripnyak. Fracture of Ceramic Materials under Dynamic Loadings. *19th European Conf. on Fracture (ECF19)*, Kazan, Russia, Paper 639, Kazan, 2012.
- [10] J. Kimberley, K.T. Ramesh, and N.P. Daphalapurkar, A Scaling law for the dynamic strength of brittle solids. *Acta Mater.*, **61**, 3509–3521, 2013.
- [11] K.T. Ramesh, J. D. Hogan, J. Kimberley, and A Stickle, A review of mechanisms and models for dynamic failure, strength, and fragmentation. *Planetary and Space Science*, **107**, 10–23, 2015.
- [12] B. Paliwal and K.T. Ramesh, Effect of crack growth dynamics on the rate sensitive behavior of hot-pressed boron carbide. *Scripta Materialia*, **57**, 481–484, 2007.